

# Barren Plateaus Beyond Observable Concentration

Zi-Shen Li,<sup>1</sup> Bujiao Wu,<sup>2,\*</sup> Xiao-Wei Li,<sup>3</sup> and Man-Hong Yung<sup>2</sup>

<sup>1</sup>Quantum Information and Computation Initiative,  
Department of Computer Science, School of Computing and Data Science,  
The University of Hong Kong, Pokfulam Road, Hong Kong, China

<sup>2</sup>International Quantum Academy, Shenzhen 518048, China

<sup>3</sup>Department of Physics, College of Physics, Chengdu University of Technology, Chengdu, 610059, China

Parameterized quantum circuits (PQCs) are central to quantum machine learning and near-term quantum simulation, but their scalability is often hindered by barren plateaus (BPs), where gradients decay exponentially with system size. Prior explanations, including expressivity, entanglement, locality, and noise, are often presented in ways that conflate two distinct issues: concentration of the measured observable and loss of parameter sensitivity caused by circuit dynamics. We develop a unified statistical framework that separates these mechanisms. We show that several standard BP explanations, including locality- and entanglement-related effects, can be understood through a single phenomenon that we term observable concentration (OC). Importantly, we prove that avoiding OC is necessary but not sufficient for trainability. Beyond OC, we identify two distinct mid-circuit sources of gradient suppression. First, mid-circuit information loss occurs when parameter perturbations propagate into degrees of freedom that are inaccessible to the final measurement, yielding little or no response. Second, mid-circuit information scrambling occurs when local perturbations rapidly spread across the system and become effectively undetectable on the measured subsystem. We support our theory with explicit constructions and numerical evidence, including quantum convolutional neural network architectures that exhibit information-loss-induced barren plateaus despite the absence of observable concentration.

## INTRODUCTION

Quantum computing faces substantial experimental and theoretical challenges. While certain quantum algorithms, such as Shor’s algorithm [1, 2], Grover’s search [3], and the HHL algorithm [4], offer provable quantum advantages, their practical realization on near-term quantum devices remains difficult. This experiment-theory gap primarily arises from the challenge of designing quantum algorithms that can simultaneously ensure provable advantages while remaining implementable on current hardware.

Parameterized quantum circuits (PQCs) have emerged as a versatile framework for demonstrating the capabilities of quantum devices, with applications spanning quantum machine learning [5–7], variational quantum eigensolvers [8–10], and quantum simulations [11–13]. A central theoretical challenge in deploying PQCs for these tasks is the phenomenon of barren plateaus (BPs). Barren plateaus manifest as exponential flatness in the training landscape, arising from various factors including entanglement [14, 15], cost function locality [16, 17], the presence of noise [18], etc. As a major obstacle to the scalability of PQCs, BPs impose an exponential overhead in the computational cost of gradient estimation. In addition, recent research has proposed several approaches to mitigate or avoid BPs, including the design of BP-free circuit architectures [19], the development of diagnostic tools for BP detection [15, 20], the formulation of training strategies to mitigate BPs [21], etc.

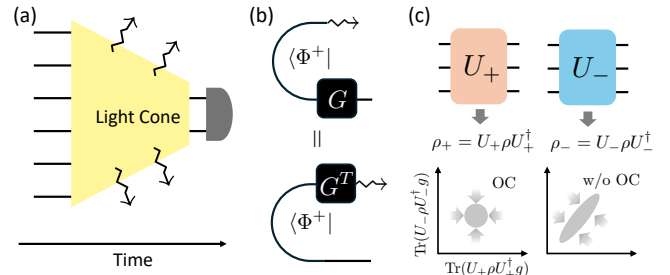


FIG. 1. Demonstration of information loss and gradient vanishing. (a) depicts information loss in variational quantum circuits. (b) shows a simple illustration on how this information loss results in vanishing response. (c) shows different statistical behaviors of BPs with and without observable concentration (OC).

Although these approaches offer a pathway to circumvent barren plateaus in PQCs, they may inadvertently imply classical simulability. This reveals a critical dilemma: mitigating barren plateaus may, in some cases, eliminate the very quantum advantage that PQCs are intended to achieve [22]. Moreover, the presence of gate noise [23] or certain types of circuit randomness [24] can also render PQCs classically simulable. In such cases, the loss function estimation becomes concentrated within a classically accessible regime, making the computation either deterministically [23, 25] or probabilistically [24] simulable. These observations naturally raise an important question: *Can a parameterized quantum circuit simultaneously exhibit quantum advantage while remaining free of barren plateaus?* To identify and characterize such regimes, it is essential to develop a deeper understanding

\* wubujiao@iqasz.cn

of the relationship between BPs and circuit architecture, necessitating a comprehensive reassessment of BPs.

A recurring ambiguity in the literature is that BP is sometimes associated not only with gradient concentration, but also with concentration of the cost (observable) values themselves. These notions coincide in many commonly studied settings, but they are not equivalent: by the parameter-shift rule, a gradient is a difference of two cost evaluations, and can therefore vanish either because each evaluation concentrates, or because the two evaluations become nearly indistinguishable due to strong correlations. We here define the *observable concentration* (OC) as the phenomenon where the variance of the observable is concentrated exponentially toward its mean. In addition, we remark that Angrisani *et al.* [24] demonstrated that local observables in certain noiseless quantum circuits can be classically estimated within acceptable mean errors. We found that this classical simulability can arise directly from OC. In this study, we explore the fundamental origins of BPs, including previously identified factors such as cost function locality [16] and entanglement [14], which we demonstrate are intrinsically linked to OC.

Our goal is to complement these end-of-circuit variance (or purity) viewpoints by making explicit an additional, operationally measurable ingredient: the parameter-shift correlation between the two shifted evaluations that define the gradient. This term is shaped by mid-circuit information dynamics and can dominate the onset of BPs even when end-of-circuit observable statistics remain non-concentrated. We formalize two mechanisms that capture this phenomenon: information loss and information scrambling.

The effect of information loss is illustrated by the toy setting in Fig. 1. If one share of a maximally entangled pair  $\Phi^+$  leaves the causal light cone of the measured region, then the perturbation induced by a local gate  $G$  is transferred into degrees of freedom that are inaccessible to the final measurement, leading to an approximately vanishing linear response. Beyond by this picture, we derive rigorous upper bounds on the gradient variance under minimal randomness assumptions. In contrast to analyses based on global Haar randomness [26], our results require only local scrambling conditions (for example, a local 2-design), which better match realistic PQC architectures.

Although information scrambling has been discussed as a potential contributor to barren plateaus, a statistical framework that cleanly separates observable concentration from scrambling-driven internal information propagation remains missing. We provide such an analysis and identify regimes where scrambling alone yields gradient suppression even when the measured subsystem remains weakly entangled. We complement the theory with explicit constructions and numerical evidence. In particular, we study a QCNN-inspired hierarchical circuit with linear depth and observe information-loss-induced barren plateaus in regimes where observable concentration is absent.

## BACKGROUND AND PRELIMINARIES

BPs reflect the trainability of parametrized quantum circuits (PQCs), which are usually considered at the ensemble level. A PQC  $U(\boldsymbol{\theta})$  is parameterized by a set of real-valued parameters  $\boldsymbol{\theta} = (\theta_1, \theta_2, \dots, \theta_m)^T$ . In the ensemble approach, we associate each unitary with a probability, i.e.,  $\mathcal{E} = \{U, p(U)\}$  and the expectation operation over this ensemble is defined as  $\mathbf{E}_{U \sim \mathcal{E}}(\cdot) := \int dU p(U)(\cdot)$ , which captures the typical behavior of the entire set of unitaries. Any specific parameterization configuration of a PQC defines an ansatz for minimizing a cost function of the form  $C(\boldsymbol{\theta}) := C[U(\boldsymbol{\theta})] := \text{Tr}[U(\boldsymbol{\theta})\rho_0 U(\boldsymbol{\theta})^\dagger H]$  where  $\rho_0$  denotes the input state, and  $H \in \mathcal{L}(\mathcal{H})$  is a Hermitian observable acting on the Hilbert space  $\mathcal{H}$ . Here,  $\mathcal{L}(\mathcal{H})$  denotes the space of linear operators acting on  $\mathcal{H}$ . The flatness of the training landscape is quantified by the variance of the gradient.

**Definition 1** (Barren plateaus). *A barren plateau (BP) arises when the gradient of the cost function, given by  $\nabla_{\boldsymbol{\theta}} C[U(\boldsymbol{\theta})] = (\partial_{\theta_1} C, \dots, \partial_{\theta_m} C)^T$  vanishes exponentially with the number of qubits  $n$  over the ensemble  $\mathcal{E}$ . Specifically, for some constant  $\alpha > 1$  and  $j \in [m]$ ,*

$$\text{Var}_{U \sim \mathcal{E}} \partial_{\theta_j} C[U(\boldsymbol{\theta})] \in \mathcal{O}(\alpha^{-n}). \quad (1)$$

This definition is an ensemble statement about typical gradients under random parameter sampling (e.g., random initialization), and it should be distinguished from the trivial fact that any landscape can contain isolated critical points with exactly zero gradient.

Although gradient-free optimization methods have been proposed [27], they encounter fundamentally equivalent challenges, as the presence of BP implies an exponentially low probability of determining the descent direction in parameter space. Therefore, without loss of generality, we focus our analysis on gradient-based approaches in this work.

We consider a system of  $n$  qubits, for which the associated Hilbert space  $\mathcal{H}$  has dimension  $d = 2^n$ . We begin by considering  $H = cg$ , where  $g$  is a local Pauli operator and  $c \in \mathbf{R}$  is a constant. Extensions to general Hamiltonians will be discussed subsequently. We assume that the ensemble  $\mathcal{E}_{\text{LS}} = \{U(\boldsymbol{\theta}), p(\boldsymbol{\theta})\}$  is *locally scrambling* [28], a property satisfied by many circuits of physical interest [24]. We give the formal definition as follows.

**Definition 2** (Locally scrambling ensemble). *The ensemble  $\mathcal{E}_{\text{LS}}$  is said to be locally scrambling if for any random unitary  $U \sim \mathcal{E}_{\text{LS}}$  and a tensor product of single-qubit Clifford gates  $\bigotimes_j V_j$ , we have  $(\bigotimes_j V_j)U \sim \mathcal{E}_{\text{LS}}$ .*

We also let the probability distribution  $p(\boldsymbol{\theta})$  be translation invariant in  $\boldsymbol{\theta}$ , which is equivalent to uniformly sampling  $\theta_j$  from  $[0, 2\pi)$ . According to the parameter shift rule [29, 30], the derivative of the cost function can be written as

$$\partial_{\theta_i} C(\boldsymbol{\theta}) = u [C(\boldsymbol{\theta} + \mathbf{e}_i \pi/4u) - C(\boldsymbol{\theta} - \mathbf{e}_i \pi/4u)], \quad (2)$$

where  $u$  is a constant that depends on the generator of the parameterized gate and  $\mathbf{e}_i$  is the  $i$ -th unit vector. Let  $\rho(\boldsymbol{\theta}) = U(\boldsymbol{\theta})\rho_0 U^\dagger(\boldsymbol{\theta})$ , and define the shifted states  $\rho_\pm(\boldsymbol{\theta}) := \rho(\boldsymbol{\theta} \pm \mathbf{e}_i \pi/4u)$ . For simplicity, we use the notation  $\rho$  and  $\rho_\pm$  to denote  $\rho(\boldsymbol{\theta})$  and  $\rho_\pm(\boldsymbol{\theta})$ , respectively. The variance can be expressed as

$$\text{Var}_{U \sim \mathcal{E}} \partial_{\theta_i} C = c^2 u^2 \mathbf{E}_{U \sim \mathcal{E}} |\text{Tr}[g\rho_+ - g\rho_-]|^2.$$

By the translation invariance of the ensemble  $\mathcal{E}$ , this expression simplifies to

$$\text{Var}_{U \sim \mathcal{E}} \partial_{\theta_i} C = 2c^2 u^2 (1-r) \mathbf{E}_{U \sim \mathcal{E}} [\text{Tr}(g\rho)]^2. \quad (3)$$

where the ratio

$$r := \mathbf{E}_{U \sim \mathcal{E}} \text{Tr}[g\rho_+] \text{Tr}[g\rho_-] / \mathbf{E}_{U \sim \mathcal{E}} [\text{Tr}(g\rho)]^2 \quad (4)$$

is the *Pearson correlation coefficient*, which quantifies the linear correlation between the measurement outcomes on the two shifted states. In certain cases,  $r$  can approach 1 exponentially with the number of qubits  $n$ , becoming a significant factor of BPs. Under local scrambling and translation invariance,  $\mathbf{E}[\text{Tr}(g\rho)] = 0$  and  $\mathbf{E}[\text{Tr}(g\rho_+)^2] = \mathbf{E}[\text{Tr}(g\rho_-)^2] = \mathbf{E}[\text{Tr}(g\rho)^2]$ , so  $r \in [-1, 1]$  is exactly the Pearson correlation coefficient between the two parameter-shift evaluations. We interpret  $(1-r)$  as a *parameter-shift distinguishability* factor:  $r \rightarrow 1$  means the two shifted circuits become statistically indistinguishable on the measured observable, leading to vanishing gradients even when  $\mathbf{E}[\text{Tr}(g\rho)^2]$  does not decay exponentially.

The quantity  $\mathbf{E}_{U \sim \mathcal{E}} [\text{Tr}(g\rho)]^2$  in Eq. (3) characterizes the variance of the observable  $g$ , given that its expectation vanishes under the locally scrambling ensemble. This term reflects the degree of concentration of measurement outcomes induced by the ensemble at the end of the circuit. While prior work [31] has attributed the vanishment in the variance of observable to BPs, the contribution of the Pearson correlation coefficient—particularly how it is affected by the inner structures of the ansatz—remains largely unexplored.

We first study when the observable second-moment factor  $\mathbf{E}[\text{Tr}(g\rho)]^2$  becomes exponentially small (observable concentration).

We begin by demonstrating how BPs can arise from concentration phenomena in end-of-circuit measurement statistics. For a locally scrambling ensemble  $\mathcal{E}$  and a state  $\rho = U\rho_0 U^\dagger$  with  $U \sim \mathcal{E}$ , we derive the following bound:

**Theorem 1** (Observable Concentration from Local Scrambling). *For a locally scrambling ensemble  $\mathcal{E}$  and a state  $\rho = U\rho_0 U^\dagger$  with  $U \sim \mathcal{E}$ , the second moment of the observable  $g$  is bounded by:*

$$\mathbf{E}_{U \sim \mathcal{E}} [\text{Tr}(g\rho)]^2 \leq \left(\frac{2}{3}\right)^{|A|} \mathbf{E}_{U \sim \mathcal{E}} D_{\text{HS}}^2(\rho_A), \quad (5)$$

where  $A = \text{supp}(g)$  denotes the support of the Pauli operator  $g$ ,  $\rho_A$  is the reduced density matrix of  $\rho$  on subsystem  $A$ , and  $D_{\text{HS}}(\rho_A) := \|\rho_A - \mathbb{1}/2^{|A|}\|_{\text{F}}$  denotes the Hilbert-Schmidt deviation between the reduced state  $\rho_A$  and the maximally mixed state on subsystem  $A$ .

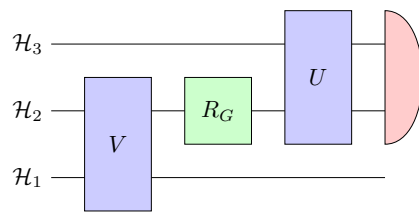


FIG. 2. Circuit models to demonstrate mid-circuit response.  $\mathcal{H}_1, \mathcal{H}_2$  and  $\mathcal{H}_3$  denote different Hilbert spaces with dimensions  $d_1, d_2$ , and  $d_3$  respectively. The measurement is taken within  $\mathcal{H}_2 \otimes \mathcal{H}_3$ .

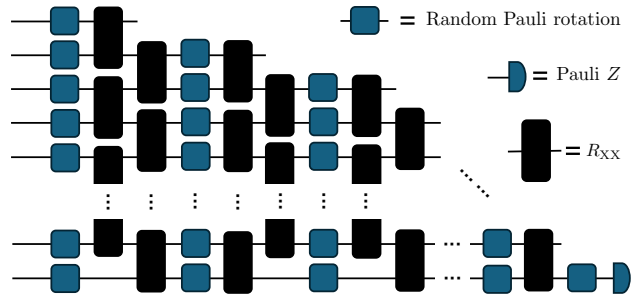


FIG. 3. Hierarchical tree circuit model (linear depth). This quantum circuit consists of  $L$  layers of single-qubit and two-qubit parameterized gates. The qubits are indexed sequentially from bottom to top, denoted as  $1, 2, \dots, n$ . Similarly, the layers are labeled consecutively from left to right, labeled as  $1, 2, \dots, L$ .

We remark that Theorem 1 significantly generalizes standard concentration results: it does not rely on the assumption of global Haar randomness or deep circuits, but requires only local scrambling. This implies that OC can occur even in shallow or intermediate-depth circuits, provided they satisfy the local scrambling property. By Theorem 1, observable concentration (OC) can be attributed to two main factors: (1) high entanglement in the end-of-circuit state, which causes the reduced state on subsystem  $A$  to approach the maximally mixed state. In the context of quantum neural networks, this effect manifests through the growth of hidden-layer dimensions [14]; and (2) the use of global cost functions [16, 32], which is indicated by the exponent  $|A|$  in Eq. (5). We also note that noise-induced BPs [18] are likely a consequence of OC, which extends beyond the scope of this work. In the following, we investigate how the internal structure of the ansatz contributes to the emergence of BPs, beyond the effects accounted for by OC.

### BPS INDUCED BY INFORMATION LOSS

As the entire process of PQC involves adaptive updates to the parameters within the circuit, a detailed examination of the mid-circuit behavior within PQC is essential. To formalize this, we analyze the derivative of a parameterized gate of the form  $\exp(-iG\theta)$ , where  $G$  is a

Pauli operator. This gate is positioned between a forward circuit block  $U$  and a backward circuit block  $V$ . The unitaries  $U$  and  $V$  are drawn from unitary ensembles  $\mathcal{E}_U$  and  $\mathcal{E}_V$ , respectively. For generality, we assume only that  $\mathcal{E}_V$  is locally scrambled, while  $\mathcal{E}_U$  remains a flexible choice within our model. We begin by considering cost functions of the form  $\text{Tr}[O\rho]$ , where  $\rho$  denotes the state prepared by the circuit, and subsequently extend the analysis to a batch-decomposed formulation.

To analyze the mid-circuit behavior of the circuit evolution, we start by examining the snapshot of the system state  $\rho_V$  immediately following the application of unitary  $V$ . Let  $\Gamma$  denote the light-cone subspace, defined as the set of qubits that back-propagate from the support of the observable through the circuit up to  $V$ . Specifically, this subspace can be expressed as  $\Gamma = \text{supp}(U^\dagger O U)$  with  $O$  being an arbitrary observable. The gradient variance is determined by the reduced state of  $\tilde{\rho}_V^{\otimes 2}$  on the light-cone region  $\Gamma$ . After simplification, we find that it admits the following upper bound

$$c^2 u^2 \|O\|_2^2 \|\mathbf{E}_{V \sim \mathcal{E}_{\text{LS}}} \text{Tr}_{\neq \Gamma}(\tilde{\rho}_V^{\otimes 2})\|_1, \quad (6)$$

where  $\tilde{\rho}_V = G\rho_V G - \rho_V$  and  $\|\cdot\|_k$  denotes the  $l_k$  norm. Further details and a full derivation of this result are provided in Methods.

Before diving into the rigorous derivation, we can gain intuition from Fig. 1 (a) and (b): strong entanglement across the light-cone boundary can transfer the effect of a local perturbation into degrees of freedom outside the measurement light cone (an entanglement-assisted ‘‘leakage’’ mechanism). In such cases, the reduced state within the light cone approaches maximally mixed, and the measurement becomes insensitive to the perturbation.

Specifically, let  $\mathcal{P}_\Gamma$  denote the set of Pauli basis on  $\Gamma$ . We define the effective Pauli set as  $S(\Gamma, G) := \{\mathbf{1}, g | g \in \mathcal{P}_\Gamma, gG + Gg = 0\}$  and introduce the effective reduced state  $\varrho_\Gamma(V) := 2^{-|\Gamma|} \sum_{g \in S(\Gamma, G)} g \text{Tr}[g\rho_\Gamma(V)]$ . The corresponding information loss is then characterized by the Hilbert-Schmidt deviation of  $\varrho_\Gamma(V)$  from the maximally mixed state. We emphasize that while  $\varrho_\Gamma$  is not generally equal to the reduced state  $\rho_\Gamma$ , it captures the specific information component recoverable by the gradient operator  $G$ . By projecting onto the subspace of operators anti-commuting with  $G$ ,  $\varrho_\Gamma$  provides a tighter bound than  $\rho_\Gamma$  for locally scrambling ensembles, serving as a more precise statistical signature of trainability.

**Theorem 2** (Information loss and barren plateaus). *Let  $O$  be an arbitrary Hermitian operator and its expectation value be the cost function. Let  $\Gamma$  denote the light cone subspace after applying the locally scrambling unitary  $V$ . The variance of the gradient is upper bounded as:*

$$\text{Var}(\partial_\theta C) \leq u^2 \|O\|_2^2 2^{|\Gamma|+2} \mathbf{E}_V D_{\text{HS}}^2[\varrho_\Gamma(V)]. \quad (7)$$

Notably, Theorem 2 does not rely on Haar randomness for either  $U$  or  $V$ ; it is sufficient that the circuit  $V$  exhibits local scrambling while remaining independent of the distribution of  $U$ . This condition highlights the irreversible

character of information loss, which cannot be remedied by any post-processing unitaries. This also suggests that BPs can emerge even in the absence of OC if we choose  $U$  carefully enough to maintain non-concentrated end-circuit statistics. Indeed, information loss provides a concrete mid-circuit mechanism to realize BPs without OC. To demonstrate this, we must isolate the factor of OC from the gradient variance, which reveals the key quantity  $r$  as shown in Eq. (3). We then present several concrete examples to elaborate on this.

Consider the circuit structure shown in Fig. 2, where the unitary  $V$  is drawn from a unitary 2-design, the operator  $G$  is a Pauli observable with support restricted within the subspace  $\mathcal{H}_2$ , i.e.,  $\text{supp}(G) \subset \mathcal{H}_2$ . We assume the initial state is a product state  $\rho_0 = \rho_{12} \otimes \rho_3$ , and  $U$  acts trivially on the partition boundary such that separability is maintained up to  $V$ . Due to the circuit geometry, only measurements performed on  $\mathcal{H}_2$  and  $\mathcal{H}_3$  can detect changes in the parameter  $\theta$ . Focusing on the snapshot of the system after applying the unitary  $V$ , the light cone subspace is  $\mathcal{H}_2 \otimes \mathcal{H}_3$  and the state can be written as  $\rho_V = \rho_V^{(1,2)} \otimes \rho_V^{(3)}$ , where the superscripts indicate different subspaces. According to Theorem 2, we obtain the effective reduced state as  $\varrho_\Gamma = 2^{-|\Gamma|} \sum_{g_i \otimes g_j \in \mathcal{P}(G, \Gamma)} g_i^{(2)} \otimes g_j^{(3)} \text{Tr}[g_i^{(2)} \rho_V^{(2)}] \text{Tr}[g_j^{(3)} \rho_V^{(3)}]$ . As the state is of product form between  $\mathcal{H}_2$  and  $\mathcal{H}_3$ , we can write the deviation in a simpler form and disregard the subsystem  $\mathcal{H}_3$  through the inequality, i.e.,  $D_{\text{HS}}^2(\varrho_\Gamma) = D_{\text{HS}}^2[\rho_V^{(2)}] \text{Tr}[\rho^{(3)2}] \leq D_{\text{HS}}^2[\rho_V^{(2)}]$ . Now the result becomes clear: the variance of gradient is connected to the Hilbert-Schmidt deviation of the reduced state in  $\mathcal{H}_2$  from the maximally mixed state, which can be easily achieved for any  $V$  that is random enough. The construction in the following example, obtained by taking  $U$  and  $V$  from a unitary 2-design, serves as a special case of Theorem 2.

**Example 1.** *For the circuit configuration shown in Fig. 2, let  $U$  and  $V$  be unitary 2-design and assume the dimensional constraint  $d_2 \leq d_3/2$ . Under these conditions, the Pearson correlation coefficient admits the bound  $1 - r = \mathcal{O}(d_2^2/d_1)$ .*

Detailed calculation can be found in Methods. As shown in Example 1, the Pearson correlation coefficient satisfies  $1 - r = \mathcal{O}(d_2^2/d_1)$ , which leads to barren plateaus with  $d_1$  increasing exponentially. Meanwhile, the variance associated with the observable scales as  $\mathcal{O}(d_2^{-2}d_3^{-1})$  and is independent of  $d_1$ . This indicates that the component of the gradient variance induced by  $d_1$  cannot be inferred from the measurement statistics of the observable alone.

In machine learning applications, training data is commonly divided into mini-batches to enhance computational efficiency and model robustness. This mini-batch learning approach has proven effective in both classical and quantum domains [33, 34]. We extend theorem 2 by introducing a decomposition of a Hermitian operator into Pauli batches. Let  $\{\mathcal{P}_j\}_{j=1}^K$  represent a partition of

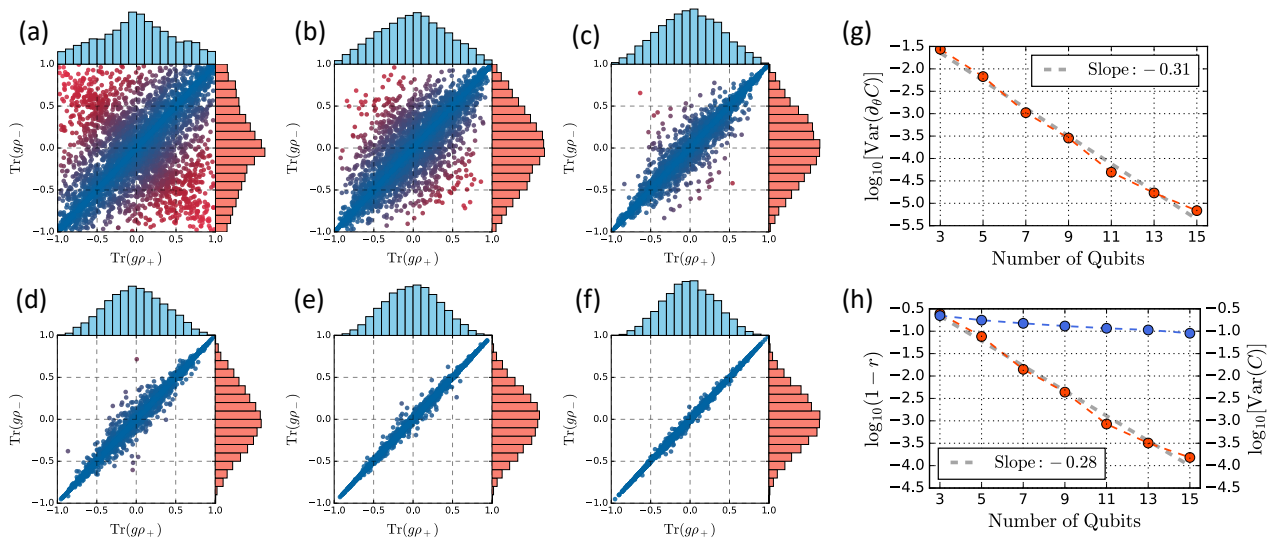


FIG. 4. Hierarchical tree-circuit trainability diagnostics via parameter-shift statistics. (a)-(f) present scatter plots of shifted terms in circuits containing 3, 5, 7, 9, 11, and 13 qubits, respectively. (g) illustrates how gradient variance vanishes with increasing number of qubits, with a gray dashed line representing the linear fit in logarithmic scale. (h) displays the comparison between  $(1 - r)$  and the observable variance, accompanied by a fitted straight line for  $(1 - r)$  in logarithmic scale as well.

the Pauli set  $\mathcal{P}$  into  $K$  disjoint subsets. For a Hermitian operator  $O$ , we define its  $K$ -Pauli batch decomposition as  $O = \sum_{j=1}^K B_j$ , where the  $j$ -th batch  $B_j = \sum_{g \in \mathcal{P}_j} c_g g$  comprises Pauli operators  $g$  with corresponding coefficients  $c_g$ . This decomposition yields the following corollary:

**Corollary 3** (Batch-decomposed form of Theorem 2). *For the cost function in the form  $C = \text{Tr}[UR_G(\theta)V\rho_0V^\dagger R_G(\theta)^\dagger U^\dagger O]$  with  $U, V \in \mathcal{E}_{\text{LS}}$  and the Hamiltonian in the  $K$ -Pauli decomposition form, i.e.,  $H = \sum_{j=1}^K B_j$ , the variance of gradient can be bounded as*

$$\text{Var}(\partial_\theta C) \leq \sum_{j=1}^K u^2 \|B_j\|_2^2 2^{|\Gamma_j|+2} \mathbf{E}_V D_{\text{HS}}^2[\partial_{\Gamma_j}(V)], \quad (8)$$

where  $\Gamma_j$  is the light-cone subspace of  $j$ -th batch, i.e.,  $\Gamma_j = \text{supp}(U^\dagger B_j U)$ .

A detailed proof of this corollary is provided in Methods.

### BPS INDUCED BY INFORMATION SCRAMBLING

We here introduce a class of BPs induced by information scrambling, which arise independently of observable concentration as well. Quantum information scrambling is a fundamental characteristic of quantum many-body dynamics, wherein local information rapidly spreads throughout the entire system [35]. This phenomenon poses a significant challenge for variational circuits, as

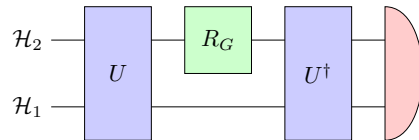


FIG. 5. Circuit models to demonstrate the impact of information scrambling on BPs. The measurement is applied within the joint space  $\mathcal{H}_1 \otimes \mathcal{H}_2$ .

the effects of parameter shifts can be scrambled and consequently harder to detect. We consider a circuit model depicted in Fig. 5. The model comprises a parameterized gate  $R_G(\theta)$  sandwiched by two layers of unitaries, i.e.,  $U$  and  $U^\dagger$ , that operate on a  $d$ -dimensional quantum system. Such architectures are widely applied in various tasks, such as unknown unitary learning, scrambling-based quantum metrology [36], and quantum autoencoders [37, 38]. For clarity we fix the probed parameter at  $\theta = 0$  (so  $R_G(\theta) = \mathbb{1}$ ) while averaging over the random unitary  $U$  (or, equivalently, over the remaining circuit parameters). This isolates scrambling-driven indistinguishability in the parameter-shift evaluations and should not be interpreted as focusing on an isolated critical point of a fixed deterministic landscape. It can be readily verified that this circuit configuration generates non-concentrated end-circuit statistics.

Our investigation reveals that when we compute the derivative of the parameterized gate at the circuit's midpoint, the derivative information becomes scrambled and exponentially less detectable. Our findings are summarized as follows.

**Example 2.** For the circuit architecture depicted in Fig. 5 with  $U$  being 4-design, the Pearson correlation coefficient satisfies  $1 - r = \mathcal{O}(\frac{1}{d})$ , and the corresponding gradient variance scales as  $1 - r$ .

The detailed calculation is presented in Methods. As anticipated, the gradient in this scenario exponentially vanishes while maintaining the observable non-concentrated. We remark that the intuition behind this is that even an infinitesimal shift in  $\theta$  will render the entire circuit into a completely random unitary, resulting in gradient vanishing. The result confirms that a generic unknown unitary is not learnable through variational circuits.

## NUMERICAL SIMULATION

We numerically test our theoretical predictions using the hierarchical tree circuit architecture in Fig. 3, which is inspired by quantum convolutional neural network (QCNN) constructions [19] but has linear depth in the number of qubits. Our purpose is therefore not to revisit QCNN trainability guarantees, but to use this controlled linear-depth hierarchical architecture to isolate the mid-circuit correlation mechanism ( $r \rightarrow 1$ ) predicted by Eq. (3).

As illustrated in Fig. 3, the circuit model comprises  $L$  layers of single-qubit gates  $R_P^{(i,j)}(x) = \exp(-ixP/2)$ , where  $P$  is randomly selected from Paulis  $\{X, Y, Z\}$ , and two-qubit gates  $R_{XX}^{(i,j)}(y) = \exp(-iyX \otimes X)$ . The indices  $(i, j)$  on the superscript indicate that the gate is applied at  $i$ -th qubit and  $j$ -th layers. The complete circuit evolution can be written as  $U_P^{(L+1)} \prod_{k=1}^L U_{XX}^{(k)} U_P^{(k)}$ , where  $U_P^{(k)} = \prod_{j=1}^{L-k+2} R_P^{(j,k)}$  and  $U_{XX}^{(k)} = \prod_{j=1}^{L-k+1} R_{XX}^{(j,k)}$ . We let the observable be the Pauli  $Z$  acting on the last register and the input state be the zero state  $|00\dots 0\rangle$ . To analyze the mid-circuit dynamics, we focus on the derivative of the central single-qubit gate, i.e.,  $R_P^{(L/2, L/2)}$ , and fix the number of layers  $L = n - 1$  with  $n$  being the number of qubits.

We sample all gate parameters independently and uniformly from  $[0, 2\pi)$  and evaluate the gradient via the parameter-shift rule, which yields two shifted terms  $\text{Tr}[g\rho_+]$  and  $\text{Tr}[g\rho_-]$ . The results are shown in Fig. 4. Panels (a)–(f) display scatter plots of  $\text{Tr}[g\rho_+]$  versus  $\text{Tr}[g\rho_-]$  (with marginal histograms) for increasing  $n$ . As  $n$  grows, the two shifted terms become increasingly linearly dependent, approaching  $\text{Tr}[g\rho_+] \approx \text{Tr}[g\rho_-]$ , which is quantified by the Pearson correlation coefficient  $r \rightarrow 1$ . Panels (g) and (h) report the gradient variance,  $r$ , and the observable variance on logarithmic scales. Notably, the decay of  $\log_{10}(1 - r)$  closely matches the decay of the gradient variance, whereas the observable variance does not exhibit a comparable decrease. This behavior indicates barren plateaus without OC, consistent with gradient suppression driven by mid-circuit information loss through the increasing correlation between the two shifted evaluations.

## CONCLUSION AND DISCUSSION

We have shown that observable concentration does not fully explain trainability issues in PQCs: the gradient variance naturally decomposes into an end-of-circuit observable second-moment term and a parameter-shift distinguishability term ( $1 - r$ ). In particular, we identify two mid-circuit mechanisms, information loss and information scrambling, that can induce BPs even when the cost function does not concentrate under random parameter sampling. This separation reveals a subtle but practically important regime: the objective may display noticeable fluctuations across random parameters, yet gradients with respect to specific parameters can be exponentially suppressed because the corresponding perturbations become inaccessible to the final measurement, or are delocalized by scrambling. From this viewpoint, BPs reflect a limitation of the circuit’s ability to transmit parameter dependence to the measured degrees of freedom, rather than solely a property of the output statistics. Because  $r$  can be estimated from the same parameter-shift evaluations used to compute gradients, it provides an experimentally accessible diagnostic of sensitivity loss that is complementary to end-of-circuit variance (or purity) diagnostics. This perspective is also complementary to Lie-algebraic and purity-based approaches: those frameworks characterize which operator directions are in principle accessible, whereas  $(1 - r)$  captures when accessible directions become practically indistinguishable due to mid-circuit information dynamics.

Our results also offer a complementary perspective on parameter redundancy and effective model capacity [39, 40]. Parameters whose influence is lost or scrambled contribute little to optimization, effectively reducing the dimensionality of the trainable parameter space even when the nominal parameter count is large.

Several directions follow naturally. First, it will be valuable to develop practical diagnostics that detect mid-circuit information loss or excessive scrambling during training, and to translate these diagnostics into architecture or initialization principles that preserve parameter sensitivity. Second, understanding the interplay with noise remains an open issue: realistic noise may further erase propagating perturbations, but it may also suppress scrambling or modify the effective causal structure in ways that are not captured by idealized models. Clarifying these effects is important for predicting trainability on hardware and for designing scalable variational algorithms that can realize reliable performance improvements.

## METHODS

### Proof of Eq. (5)

*Proof.* We first write the output state in the Pauli basis:

$$\rho = U(\boldsymbol{\theta})\rho_0U(\boldsymbol{\theta})^\dagger = \frac{1}{d} \left( \mathbb{1} + \sum_{k=1}^{d^2-1} \lambda_k g_k \right), \quad (9)$$

where  $\mathbb{1}$  is the identity operator,  $\{g_k\}$  are the Pauli operators, and  $\lambda_k \in \mathbf{R}$  are expectation values of the Pauli operators, i.e.,  $\lambda_k = \text{Tr}(\rho g_k)$ . Then we have

$$\mathbf{E}_{U \sim \mathcal{E}} \lambda_k^2 = \mathbf{E}_{U \sim \mathcal{E}} [\text{Tr}(g_k U \rho_0 U^\dagger)]^2, \quad (10)$$

which can be further written as follows, according to the locally scrambling properties:

$$\mathbf{E}_{U \sim \mathcal{E}} \text{Tr}(g_k^{\otimes 2} \rho^{\otimes 2}) = \mathbf{E}_{U \sim \mathcal{E}} \text{Tr}(C^{\dagger \otimes 2} g_k^{\otimes 2} C^{\otimes 2} \rho^{\otimes 2}), \quad (11)$$

with  $C$  being a tensor product of arbitrary single-qubit Clifford operations. The single-qubit Clifford operations can map the operator  $g$  to arbitrary Pauli operators while preserving its support. We then have

$$\begin{aligned} \mathbf{E}_{U \sim \mathcal{E}} \text{Tr}(\rho^2) &= \frac{1}{d} \left[ 1 + \sum_{k=1}^{d^2-1} \mathbf{E}_{\mathcal{E}} (\lambda_k^2) \right] \quad (12) \\ &= \frac{1}{d} \left[ 1 + \sum_{S \subset [n]} \sum_{k: \text{supp}(g_k)=S} \mathbf{E}_{\mathcal{E}} (\lambda_k^2) \right], \quad (13) \end{aligned}$$

where all the  $\mathbf{E}_{\mathcal{E}} (\lambda_k^2)$  with  $\text{supp}(g_k) = S$  must have the same average. We then have

$$\mathbf{E}_{U \sim \mathcal{E}} \text{Tr}(\rho^2) = \frac{1}{d} \left[ 1 + \sum_{S \subset [n]} 3^{|S|} \mathbf{E}_{\mathcal{E}} (\lambda_S^2) \right]. \quad (14)$$

Let  $A = \text{supp}(g)$ , and we have

$$\mathbf{E}_{U \sim \mathcal{E}} \text{Tr}(\rho_A^2) = \frac{1}{d_A} \left[ 1 + \sum_{S \subset A} 3^{|S|} \mathbf{E}_{\mathcal{E}} (\lambda_S^2) \right] \quad (15)$$

$$\geq \frac{1}{d_A} \left[ 1 + 3^{|A|} \mathbf{E}_{\mathcal{E}} (\lambda_A^2) \right]. \quad (16)$$

The expectation value of  $g$  can be bounded as

$$\mathbf{E}_{U \sim \mathcal{E}} [\text{Tr}(g\rho)]^2 \leq \frac{d_A \mathbf{E}_{U \sim \mathcal{E}} \text{Tr}(\rho_A^2) - 1}{3^{|\text{supp}(g)|}}. \quad (17)$$

□

### Proof of Eq. (6)

*Proof.* Let  $\tilde{\rho}_V = G\rho_V G - \rho_V$  and the gradient variance can be written as

$$\text{Var}_{U, V \sim \mathcal{E}} \partial_\theta C = c^2 u^2 \text{Tr} [\mathbf{E}_{U, V} g^{\otimes 2} (U \tilde{\rho}_V U^\dagger)^{\otimes 2}] \quad (18)$$

$$= c^2 u^2 \text{Tr} [\mathbf{E}_{U, V} (U^\dagger g U)^{\otimes 2} \tilde{\rho}_V^{\otimes 2}]. \quad (19)$$

We let  $\Gamma$  denote the light-cone subspace at the snapshot  $\rho_V$ , which can be defined by the support of the operator  $U^\dagger g U$ . We can then relax the bound by introducing an operator  $M_\Gamma$  with support  $\Gamma$ :

$$\begin{aligned} &\text{Tr} [\mathbf{E}_{U, V} (U^\dagger g U)^{\otimes 2} \tilde{\rho}_V^{\otimes 2}] \\ &\leq \sup_{\|M_\Gamma\|_2 \leq 1} \|g\|_2^2 \text{Tr} (M_\Gamma^{\otimes 2} \mathbf{E}_V \tilde{\rho}_V^{\otimes 2}) \quad (20) \end{aligned}$$

$$= \sup_{\|M_\Gamma\|_2 \leq 1} \|g\|_2^2 \text{Tr} (M_\Gamma^{\otimes 2} \mathbf{E}_V \text{Tr}_{\neq \Gamma} \tilde{\rho}_V^{\otimes 2}) \quad (21)$$

$$\leq \sup_{\|M'_\Gamma\|_2 \leq 1} \|g\|_2^2 \text{Tr} (M'_\Gamma \mathbf{E}_V \text{Tr}_{\neq \Gamma} \tilde{\rho}_V^{\otimes 2}) \quad (22)$$

$$= \|g\|_2^2 \|\mathbf{E}_V \text{Tr}_{\neq \Gamma} \tilde{\rho}_V^{\otimes 2}\|_1. \quad (23)$$

The second inequality arises from relaxing  $M_\Gamma^{\otimes 2}$  to  $M'_\Gamma$ , where  $M'_\Gamma$  is an operator with support on  $\Gamma^{\otimes 2}$ . □

### Proof of Theorem 2

*Proof.* According to Eq. (6), the gradient variance can be upper bounded by evaluating the trace norm of the quantity  $\mathbf{E}_V \text{Tr}_{\neq \Gamma} \tilde{\rho}_V^{\otimes 2}$ .

We first expand  $\tilde{\rho}_V^{\otimes 2}$ :

$$\tilde{\rho}_V^{\otimes 2} = (G\rho_V G - \rho_V)^{\otimes 2} \quad (24)$$

$$= \frac{1}{d^2} \left[ \sum_j \lambda_j (G g_j G - g_j) \right]^{\otimes 2} \quad (25)$$

$$= \frac{1}{d^2} \left( \sum_{j: [g_j, G] \neq 0} \lambda_j \times 2g_j \right)^{\otimes 2} \quad (26)$$

$$= \frac{4}{d^2} \sum_{i, j: [g_{i,j}, G] \neq 0} \lambda_i \lambda_j (g_i \otimes g_j), \quad (27)$$

where  $g_{i,j}$  is used as shorthand to indicate either  $g_i$  or  $g_j$ , with a slight abuse of notation. Here we use the expanded form of  $\rho_V = (\mathbb{1} + \sum_j g_j \lambda_j)/d$ . As the partial trace operation will eliminate most of the terms in  $\{g_i \otimes g_j\}$ , we can simplify this by defining the Pauli set  $\mathcal{P}_{\text{eff}} := \{g | g \in \mathcal{P}_\Gamma, gG + Gg = 0\}$ . We then have

$$\text{Tr}_{\neq \Gamma} \tilde{\rho}_V^{\otimes 2} = \frac{4}{4^{|\Gamma|}} \sum_{i, j: g_{i,j} \in \mathcal{P}_{\text{eff}}} \lambda_i \lambda_j (g_i \otimes g_j). \quad (28)$$

Now we compute the ensemble average in the above equation. As the ensemble of  $V$  is locally scrambled, we can ignore the cross terms as they do not contribute to the average:

$$\mathbf{E}_V \text{Tr}_{\neq \Gamma} \tilde{\rho}_V^{\otimes 2} = \frac{4}{4^{|\Gamma|}} \sum_{j: g_j \in \mathcal{P}_{\text{eff}}} g_j^{\otimes 2} \mathbf{E}_V \lambda_j^2. \quad (29)$$

We need to evaluate the trace norm that should be upper bounded by the Frobenius norm through the C-S

inequality:

$$\|\mathbf{E}_V \text{Tr}_{\neq \Gamma} \tilde{\rho}_V^{\otimes 2}\|_1 \leq 2^{|\Gamma|} \|\mathbf{E}_V \text{Tr}_{\neq \Gamma} \tilde{\rho}_V^{\otimes 2}\|_{\mathbb{F}}. \quad (30)$$

We further expand it to obtain:

$$\|\mathbf{E}_V \text{Tr}_{\neq \Gamma} \tilde{\rho}_V^{\otimes 2}\|_{\mathbb{F}} = \frac{4}{4^{|\Gamma|}} \left\| \sum_{j: g_j \in \mathcal{P}_{\text{eff}}} g_j^{\otimes 2} \mathbf{E}_V \lambda_j^2 \right\|_{\mathbb{F}} \quad (31)$$

$$= \frac{4}{4^{|\Gamma|}} \sqrt{\sum_{j: g_j \in \mathcal{P}_{\text{eff}}} 4^{|\Gamma|} (\mathbf{E}_V \lambda_j^2)^2} \quad (32)$$

$$\leq \frac{4}{4^{|\Gamma|}} \sum_{j: g_j \in \mathcal{P}_{\text{eff}}} 2^{|\Gamma|} \mathbf{E}_V \lambda_j^2 \quad (33)$$

$$= 4D_{\text{HS}}^2[\varrho_{\Gamma}(V)]. \quad (34)$$

Here  $\varrho_{\Gamma}(V) = \mathbf{1}_{\Gamma}/2^{|\Gamma|} + \sum_{j: g_j \in \mathcal{P}_{\text{eff}}} \lambda_j g_j/2^{|\Gamma|}$ . To conclude,

$$\text{Var}_{U,V \sim \mathcal{E}} \partial_{\theta_i} C \leq c^2 u^2 \|g\|_2^2 2^{|\Gamma|} \|\mathbf{E}_V \text{Tr}_{\neq \Gamma} \tilde{\rho}_V^{\otimes 2}\|_{\mathbb{F}} \quad (35)$$

$$\leq c^2 u^2 \|g\|_2^2 2^{|\Gamma|+2} \mathbf{E}_V D_{\text{HS}}^2[\varrho_{\Gamma}(V)]. \quad (36)$$

□

### Calculation of Example 1

Consider unitary of a circuit acting on the composite Hilbert space  $\mathcal{H}_1 \otimes \mathcal{H}_2 \otimes \mathcal{H}_3$  with dimensions  $d_1, d_2$ , and  $d_3$ , having the form  $U_{(2,3)} e^{-iG_{[2]}\theta} V_{(1,2)}$ , where the indices  $(i, j, \dots)$  denote the labels of supports of the operators, i.e.,  $O_{(i,j,\dots)} = \mathbf{1}_{\neq i,j,\dots} \otimes O$ . The measurement observable is  $g_{[2,3]}$  and the generator of the parameterized gate  $G_{[2]}$ , where the indices  $[i, j, \dots]$  denotes the support of the operator is a subset of the spaces labeled by  $(i, j, \dots)$ . Specifically,  $\text{supp}(X_{(i,j,\dots)}) = \mathcal{H}_i \otimes \mathcal{H}_j \otimes \dots$  and  $\text{supp}(X_{[i,j,\dots]}) \subset \mathcal{H}_i \otimes \mathcal{H}_j \otimes \dots$ . In this example,  $U$  and  $V$  are chosen from 2-design unitary ensembles, which we denote as  $U \sim \mathcal{E}_{2-d}$  and  $V \sim \mathcal{E}_{2-d}$  respectively. For conciseness, we will ignore the notion of  $\mathcal{E}_{2-d}$  in the following calculations.

The quantum circuit in Example 1 can be expressed as  $U_{(2,3)} e^{-iG_{[2]}\theta} V_{(1,2)}$ , where the subscript notation  $A_{(i_1, \dots, i_\ell)}$  with  $1 \leq i_1 < \dots < i_\ell \leq 3$  and  $1 \leq \ell \leq 3$  denotes an  $n$ -qubit operator that acts non-trivially only on Hilbert space  $\{\mathcal{H}_{i_1}, \dots, \mathcal{H}_{i_\ell}\}$ . Here, *nontrivially* means that the operator acts as the identity on all other qubits. Similarly,  $A_{[i_1, \dots, i_\ell]}$  denotes an operator supported on the Hilbert space  $\{i_1, \dots, i_\ell\}$ .

We use the Heisenberg picture and first calculate the average in  $g$ . According to Weingarten's calculus, we have

$$\mathbf{E}_U U_{(2,3)}^{\dagger \otimes 2} g_{[2,3]}^{\otimes 2} U_{(2,3)}^{\otimes 2} = b_U \mathbf{1} + c_U \mathbb{F}_{(2,3)}, \quad (37)$$

with the coefficients being

$$b_U = \frac{-1}{d_{23}^2 - 1}, \quad c_U = \frac{d_{23}}{d_{23}^2 - 1}. \quad (38)$$

To calculate the average in  $[\text{Tr}(\rho g)]^2$ , we have

$$\mathbf{E}_{U,V} V_{(1,2)}^{\dagger \otimes 2} U_{(2,3)}^{\dagger \otimes 2} g_{[2,3]}^{\otimes 2} U_{(2,3)}^{\otimes 2} V_{(1,2)}^{\otimes 2} \quad (39)$$

$$= b_U \mathbf{1} + c_U \mathbf{E}_V V_{(1,2)}^{\dagger \otimes 2} \mathbb{F}_{(2,3)} V_{(1,2)}^{\otimes 2}, \quad (40)$$

where the second term reduces to

$$\mathbf{E}_V V_{(1,2)}^{\dagger \otimes 2} \mathbb{F}_{(2,3)} V_{(1,2)}^{\otimes 2} = b_V \mathbb{F}_{(3)} + c_V \mathbb{F}_{(1,2,3)}, \quad (41)$$

with the coefficients being

$$b_V = \frac{d_1^2 d_2 - d_2}{d_{12}^2 - 1}, \quad c_V = \frac{d_1 d_2^2 - d_1}{d_{12}^2 - 1}. \quad (42)$$

Then we have

$$\mathbf{E}_{U,V} [\text{Tr}(\rho g)]^2 = \mathbf{E}_{U,V} \text{Tr}(\rho^{\otimes 2} g^{\otimes 2}) \quad (43)$$

$$= \text{Tr}[\rho_0^{\otimes 2} (b_U \mathbf{1} + c_U b_V \mathbb{F}_{(3)} + c_U c_V \mathbb{F}_{(1,2,3)})] \quad (44)$$

$$= b_U + c_U b_V \text{Tr}[\rho_0^{\otimes 2} \mathbb{F}_{(3)}] + c_U c_V \text{Tr}[\rho_0^{\otimes 2} \mathbb{F}_{(1,2,3)}] \quad (45)$$

$$= b_U + c_U b_V \text{Tr}[\rho_{0(3)}^2] + c_U c_V \text{Tr}[\rho_0^2]. \quad (46)$$

Let  $\mathbb{D} = \sqrt{G_{[2]}} \otimes \sqrt{G_{[2]}}^\dagger$ , we have

$$\mathbf{E}_{U,V} V_{(1,2)}^{\dagger \otimes 2} \mathbb{D} U_{(2,3)}^{\dagger \otimes 2} g_{[2,3]}^{\otimes 2} \mathbb{D}^\dagger U_{(2,3)}^{\otimes 2} V_{(1,2)}^{\otimes 2} \\ = b_U \mathbf{1} + c_U \mathbf{E}_V V_{(1,2)}^{\dagger \otimes 2} \mathbb{D} \mathbb{F}_{(2,3)} \mathbb{D}^\dagger V_{(1,2)}^{\otimes 2}, \quad (47)$$

where the second term reduces to

$$\mathbf{E}_V V_{(1,2)}^{\dagger \otimes 2} \mathbb{D} \mathbb{F}_{(2,3)} \mathbb{D}^\dagger V_{(1,2)}^{\otimes 2} = b'_V \mathbb{F}_{(3)} + c'_V \mathbb{F}_{(1,2,3)}, \quad (48)$$

with the coefficients being

$$b'_V = \frac{d_1^2 d_2}{d_{12}^2 - 1}, \quad c'_V = \frac{-d_1}{d_{12}^2 - 1}. \quad (49)$$

We have

$$\mathbf{E}_{U,V} \text{Tr}(\rho_+ g) \text{Tr}(\rho_- g) = \mathbf{E}_{U,V} \text{Tr}(\rho^{\otimes 2} g^{\otimes 2}) \quad (50)$$

$$= \text{Tr}[\rho_0^{\otimes 2} (b_U \mathbf{1} + c_U b'_V \mathbb{F}_{(3)} + c_U c'_V \mathbb{F}_{(1,2,3)})] \quad (51)$$

$$= b_U + c_U b'_V \text{Tr}[\rho_0^{\otimes 2} \mathbb{F}_{(3)}] + c_U c'_V \text{Tr}[\rho_0^{\otimes 2} \mathbb{F}_{(1,2,3)}] \quad (52)$$

$$= b_U + c_U b'_V \text{Tr}[\rho_{0(3)}^2] + c_U c'_V \text{Tr}[\rho_0^2]. \quad (53)$$

Combine Eqs. (38), (42), (46), (49) and (53), we have

$$1 - r \approx \frac{d_2^2 d_3 d_1 d_2}{d_1 d_2^3 d_3 - d_1^2 d_2^2 + d_1^2 d_2 d_3}, \quad (54)$$

where assume the initial state  $\rho_0$  to be a product pure state. If, in addition, the dimensional constraint  $d_2 \leq d_3/2$  holds, then the Pearson correlation coefficient satisfies

$$1 - r = \mathcal{O}\left(\frac{d_2^2}{d_1}\right). \quad (55)$$

### Proof of Corollary 3

*Proof of Corollary 3.* Let  $W = UR_G(\theta)V$  and rewrite the output state as  $\rho_W$ . We first write the cost function in the Pauli decomposition form  $C = \text{Tr}(\rho_W H) = \sum_{j=1}^L c_j C_j$ , where  $C_j = \text{Tr}(\rho_W g_j)$  and  $\{g_j\}$  are Pauli operators. The variance of the gradient can also be expanded component-wise accordingly:

$$\text{Var}_{W \sim \mathcal{E}} \left[ \sum_j c_j \partial_\theta \text{Tr}(\rho_W g_j) \right] \quad (56)$$

$$= \sum_{j,k} u^2 \mathbf{E}_{W \sim \mathcal{E}_{\text{LS}}} c_j c_k \text{Tr}[(\rho_+ - \rho_-) g_j] \text{Tr}[(\rho_+ - \rho_-) g_k] \quad (57)$$

$$= \sum_{j,k} u^2 \mathbf{E}_{W \sim \mathcal{E}_{\text{LS}}} c_j c_k \text{Tr}[(\rho_+ - \rho_-)^{\otimes 2} g_j \otimes g_k]. \quad (58)$$

Here  $\rho_\pm$  are parameter shifts of  $\rho_W$  on the parameter  $\theta$ . By switching to the Heisenberg picture and applying the trick of Pauli-mixing [24], we have

$$\mathbf{E}_{W \sim \text{Cl}(2)^{\otimes n}} W^{\dagger \otimes 2} (g_j \otimes g_k) W^{\otimes 2} = 0 \quad \text{if } j \neq k, \quad (59)$$

with  $W$  being a tensor product of arbitrary single-qubit Clifford gates. This leads to

$$\mathbf{E}_{W \sim \text{Cl}(2)^{\otimes n}} W^{\dagger \otimes 2} (B_j \otimes B_k) W^{\otimes 2} = 0 \quad \text{if } j \neq k. \quad (60)$$

We then have

$$\text{Var}_{U \sim \mathcal{E}} \partial_\theta C = \sum_{j=1}^K u^2 \text{Tr}[(\rho_+ - \rho_-)^{\otimes 2} B_j^{\otimes 2}]. \quad (61)$$

This reduces to a linear combination of the Pauli batches, where Theorem 2 can be applied individually. This completes the proof.  $\square$

### Calculation of Example 2

The coefficient  $r$  is defined as the linear dependence between  $\text{Tr}(\rho_+ g)$  and  $\text{Tr}(\rho_- g)$ , which can be further written in the vectorization form:

$$r = \frac{\mathbf{E}_{U \sim \mathcal{E}} \langle \psi |^{\otimes 4} (U \otimes U^*)^{\otimes 2} Q' (U \otimes U^*)^{\otimes 2} |g\rangle \rangle^{\otimes 2}}{\mathbf{E}_{U \sim \mathcal{E}} \langle \psi |^{\otimes 4} (U \otimes U^*)^{\otimes 2} P' (U \otimes U^*)^{\otimes 2} |g\rangle \rangle^{\otimes 2}}. \quad (62)$$

where  $P', Q' \in \mathcal{L}(\mathcal{H}_{1234})$  are operators acting on the whole space. We use the subscripts 1, 2, 3, and 4 to denote the 4 copies of the Hilbert space, and each has the dimension  $d$ . Specifically,  $P' = \sqrt{G} \otimes \sqrt{G}^* \otimes \sqrt{G} \otimes \sqrt{G}^*$  and  $Q' = \sqrt{G} \otimes \sqrt{G}^* \otimes \sqrt{G}^\dagger \otimes \sqrt{G}^T$ . Then we have

$$r = \frac{\mathbf{E}_{U \sim \mathcal{E}} \langle \psi |^{\otimes 4} [U^{\otimes 4} Q U^{\dagger \otimes 4}]^{T_{24}} |g\rangle \rangle^{\otimes 2}}{\mathbf{E}_{U \sim \mathcal{E}} \langle \psi |^{\otimes 4} [U^{\otimes 4} P U^{\dagger \otimes 4}]^{T_{24}} |g\rangle \rangle^{\otimes 2}}, \quad (63)$$

where the notion  $(\cdot)^{T_{ab}}$  represent the partial transpose on the subspaces labeled by  $a$  and  $b$ . Here  $P = P'^{T_{24}}$  and  $Q = Q'^{T_{24}}$ . Explicitly,  $P = \sqrt{G} \otimes \sqrt{G}^\dagger \otimes \sqrt{G} \otimes \sqrt{G}^\dagger$  and  $Q = \sqrt{G} \otimes \sqrt{G}^\dagger \otimes \sqrt{G}^\dagger \otimes \sqrt{G}$ . We first focus on calculating the denominator. According to Weingarten calculus, the 4-th moment can be written as

$$\mathbf{E}_{U \sim \mu_H} (U^{\otimes 4} P U^{\dagger \otimes 4}) = \sum_{\pi, \sigma \in S_4} \text{Wg}(\pi^{-1} \sigma) \text{Tr}(V_\sigma P) V_\pi, \quad (64)$$

where  $V_\pi$  is the matrix representation of the permutation  $\pi$  and  $S_4$  is a finite symmetric group with 4 elements.  $\text{Wg}(\cdot)$  is known as Weingarten function. Here we want to analyse the asymptotic behavior of the average, therefore, it is unnecessary to exactly calculate this. We only need to focus on its leading order. The leading order is contributed by the terms that satisfy  $\pi^{-1} \sigma = \text{id}$  (see [] for a comprehensive explanation).

$$\mathbf{E}_{U \sim \mu_H} (U^{\otimes 4} P U^{\dagger \otimes 4}) = \frac{1}{d^4} \sum_{\pi \in S_4} \text{Tr}(V_\pi P) V_{\pi^{-1}} \quad (65)$$

$$+ \frac{1}{d^4} \sum_{\sigma, \pi \in S_k} c_{\sigma, \pi} \text{Tr}(V_\sigma P) V_\pi. \quad (66)$$

where  $c_{\sigma, \pi}$  are  $O(1/d)$ . This inequality also holds for  $Q$ . Therefore, the calculation of the numerator will be almost the same as the denominator. As the operator  $G$  is Pauli operator, we can observe that the value of  $\text{Tr}(V_\pi P)$  satisfies the following inequality

$$\text{Tr}(V_\pi P) \leq d^{\#\text{cycle}(\pi)}. \quad (67)$$

For  $\pi = \text{id}$ , we have  $\text{Tr}(V_\pi P) = [\text{Tr}(\sqrt{G})]^4 = d^4/4$ , which gives the leading order among all the other permutations as the number of cycles reaches the maximum only in this case. As the identity is its own inverse, we have

$$\mathbf{E}_{U \sim \mathcal{E}_{\text{Haar}}} (U^{\otimes 4} P U^{\dagger \otimes 4}) = \frac{1}{4} \mathbf{1} + O(d^{-1}). \quad (68)$$

This conclusion holds for operator  $Q$  as well, i.e.,

$$\mathbf{E}_{U \sim \mathcal{E}_{\text{Haar}}} (U^{\otimes 4} Q U^{\dagger \otimes 4}) = \frac{1}{4} \mathbf{1} + O(d^{-1}). \quad (69)$$

Because there is another partial transpose on the permutation operator, it is necessary to analyze the terms in  $O(d^{-1})$  as the contraction with the state  $\psi$  and the measurement operator  $g$  can contribute at most  $O(d)$ . This can be seen by taking the inner product  $\langle\langle g | g \rangle\rangle$ . To see why this contraction is valid, we can first consider the following contractions

$$\langle \psi |^{\otimes 4} V_{\pi_1}^{T_{24}} |g\rangle \rangle^{\otimes 2} = \begin{array}{c} \text{---} \psi \\ \text{---} \psi \\ \text{---} \psi \\ \text{---} \psi \end{array} \left[ \begin{array}{c} \text{---} g \\ \text{---} g \end{array} \right] = d, \quad (70)$$

or

$$\langle \psi |^{\otimes 4} V_{\pi_2}^{T_{24}} |g\rangle \rangle^{\otimes 2} = \begin{array}{c} \psi \\ \psi \\ \psi \\ \psi \end{array} \begin{array}{c} \boxed{g} \\ \boxed{g} \end{array} = d. \quad (71)$$

We can obtain the explicit form of  $V_\pi$  by taking the partial transpose on the middle part:

$$V_{\pi_1} = \left( \begin{array}{c} \boxed{\quad} \\ \boxed{\quad} \end{array} \begin{array}{c} \boxed{\quad} \\ \boxed{\quad} \end{array} \right)^{T_{24}} = \begin{array}{c} \diagup \\ \diagdown \end{array} \Rightarrow (14)(23), \quad (72)$$

and

$$V_{\pi_2} = \left( \begin{array}{c} \boxed{\quad} \\ \boxed{\quad} \end{array} \begin{array}{c} \boxed{\quad} \\ \boxed{\quad} \end{array} \right)^{T_{24}} = \begin{array}{c} \diagup \\ \diagdown \end{array} \Rightarrow (1234). \quad (73)$$

These are only two cases where the term  $\langle \psi |^{\otimes 4} V_\pi |g\rangle \rangle^{\otimes 2}$  contributes  $O(d)$ . It can be easily verified by considering the following inner product:

$$\begin{array}{c} \boxed{g} \\ \boxed{g} \end{array}, \quad (74)$$

which fails to become a valid permutation when taking a partial transpose on the subsystems 2 and 4. The other cases where a single operator  $g$  in a loop are all zero as  $g$  is traceless. To evaluate the contribution from  $\pi_1$  and  $\pi_2$ , we can write the values of Weingarten function in different orders of  $d$  [41],

$$\text{Wg}(\pi^{-1}\sigma) = \frac{(-1)^{|\pi^{-1}\sigma|}}{d^{k+|\pi^{-1}\sigma|}} \sum_{j=0}^{\infty} \frac{\vec{W}_j(\pi, \sigma)}{d^{2j}}, \quad (75)$$

where the norm  $|\cdot|$  is the word norm corresponding to the generating set of the transpositions defined as  $|\pi| = k - \#\text{cycle}(\pi)$ .  $\vec{W}_j$  is the number of weakly monotone walks on  $S_k$  from  $\pi$  to  $\sigma$  of length  $|\pi^{-1}\sigma| + 2j$ . The leading order  $\vec{W}_0$  can be evaluated by the formula:

$$\vec{W}_0(\pi, \sigma) = \prod_{j=1}^{l(\alpha)} \frac{1}{\alpha_j} \binom{2\alpha_j - 2}{\alpha_j}, \quad (76)$$

where  $\alpha$  is the cycle type of  $\pi^{-1}\sigma$ . In our case, the permutation  $\sigma$  is set to be identity as the term  $\text{Tr}(V_{\text{id}}P) = O(d^4)$  gives the leading order. Then we can calculate the dominant term of the Weingarten function in the two cases  $\pi = \pi_1$  or  $\pi_2$ .

*Case 1.* When  $\pi = \pi_1 = (14)(23)$ , the norm  $|\pi_1^{-1}\sigma| = |\pi_1^{-1}| = k - \#\text{cycle}(\pi) = 2$ .

$$\text{Wg}(\pi_1^{-1}\text{id}) = \frac{(-1)^2}{d^{4+2}} \vec{W}_0(\pi_1, \text{id}) + O(d^{-8}). \quad (77)$$

The cycle type of  $(14)(23)$  is  $(2, 2)$ . Then we have

$$\vec{W}_0(\pi_1, \text{id}) = \left[ \frac{1}{2} \binom{2 \times 2 - 2}{2} \right]^2 = \frac{1}{4}. \quad (78)$$

The contribution of Weingarten function from this permutation is

$$\text{Wg}(\pi_1^{-1}\text{id}) = \frac{1}{4d^6} + O(d^{-8}). \quad (79)$$

Combined with the other terms, we can write the contribution to the final average as

$$\text{Wg}(\pi_1^{-1}\text{id}) \text{Tr}(V_{\text{id}}P) \langle \psi |^{\otimes 4} V_{\pi_1}^{T_{24}} |g\rangle \rangle^{\otimes 2} \quad (80)$$

$$= \frac{1}{4d^6} \times \frac{d^4}{4} \times d + O(d^{-3}) = \frac{1}{16d} + O(d^{-3}). \quad (81)$$

*Case 2.* When  $\pi = \pi_2 = (1234)$ , the norm  $|\pi_2^{-1}\sigma| = |\pi_2^{-1}| = k - \#\text{cycle}(\pi_2) = 4 - 1 = 3$ .

$$\text{Wg}(\pi_2^{-1}\text{id}) = \frac{(-1)^3}{d^{4+3}} \vec{W}_0(\pi_2, \text{id}) + O(d^{-9}). \quad (82)$$

The cycle type of  $(1234)$  is  $(4)$ . Then we have

$$\vec{W}_0(\pi_2, \text{id}) = \frac{1}{4} \binom{2 \times 4 - 2}{4} = \frac{15}{4}. \quad (83)$$

The contribution of Weingarten function from this permutation is

$$\text{Wg}(\pi_1^{-1}\text{id}) = -\frac{15}{4d^7} + O(d^{-9}). \quad (84)$$

Combined with the other terms, we can write the contribution to the final average as

$$\text{Wg}(\pi_2^{-1}\text{id}) \text{Tr}(V_{\text{id}}P) \langle \psi |^{\otimes 4} V_{\pi_2}^{T_{24}} |g\rangle \rangle^{\otimes 2} \quad (85)$$

$$= -\frac{15}{4d^7} \times \frac{d^4}{4} \times d + O(d^{-4}) = -\frac{15}{16d^2} + O(d^{-4}). \quad (86)$$

From these two cases, we can conclude that even if the order is lifted by the inner product  $\langle\langle g|g \rangle\rangle$ , the dominant term is still contributed by the identity part, which is  $O(1)$ . This analysis holds true for  $Q$  as well, with only small corrections on the higher-order terms. Therefore, we can conclude that the Pearson correlation coefficient  $r$  should satisfy the following equation:

$$r = 1 + O\left(\frac{1}{d}\right). \quad (87)$$

## DATA AVAILABILITY

Data generated and analyzed during current study are available from the corresponding author upon reasonable request.

## CODE AVAILABILITY

Code used to generate data in this study are available from the corresponding author upon reasonable request.

## ACKNOWLEDGEMENTS

This work is supported by the National Natural Science Foundation of China Grant No. 12405014, Guangdong Provincial Quantum Science Strategic Initiative (project GDZX2403008), and the General Research Fund (GRF) grant 17303923.

## AUTHOR CONTRIBUTIONS

X.-W.L. and M.-H.Y. conceived the project. Z.-S.L. and B.W. drafted the manuscript text and derived the theoretical results. X.-W.L. contributed to the analysis and discussion of the results. M.-H.Y. revised the manuscript. All authors approved the final version of the manuscript.

## COMPETING INTERESTS

The authors declare no competing interests.

- 
- [1] P. W. Shor, *SIAM Journal on Computing* **26**, 1484 (1997).
- [2] T. Monz, D. Nigg, E. A. Martinez, M. F. Brandl, P. Schindler, R. Rines, S. X. Wang, I. L. Chuang, and R. Blatt, *Science* **351**, 1068 (2016).
- [3] L. K. Grover, in *Proceedings of the Twenty-Eighth Annual ACM Symposium on Theory of Computing, STOC '96* (Association for Computing Machinery, New York, NY, USA, 1996) pp. 212–219.
- [4] A. W. Harrow, A. Hassidim, and S. Lloyd, *Physical Review Letters* **103**, 150502 (2009).
- [5] J. Biamonte, P. Wittek, N. Pancotti, P. Rebentrost, N. Wiebe, and S. Lloyd, *Nature* **549**, 195 (2017).
- [6] M. Schuld and N. Killoran, *Physical Review Letters* **122**, 040504 (2019).
- [7] J. J. Meyer, M. Mularski, E. Gil-Fuster, A. A. Mele, F. Arzani, A. Wilms, and J. Eisert, *PRX Quantum* **4**, 010328 (2023).
- [8] A. Peruzzo, J. McClean, P. Shadbolt, M.-H. Yung, X.-Q. Zhou, P. J. Love, A. Aspuru-Guzik, and J. L. O'Brien, *Nature Communications* **5**, 4213 (2014).
- [9] A. Kandala, A. Mezzacapo, K. Temme, M. Takita, M. Brink, J. M. Chow, and J. M. Gambetta, *Nature* **549**, 242 (2017).
- [10] J. Carolan, M. Mohseni, J. P. Olson, M. Prabhu, C. Chen, D. Bunandar, M. Y. Niu, N. C. Harris, F. N. C. Wong, M. Hochberg, S. Lloyd, and D. Englund, *Nature Physics* **16**, 322 (2020).
- [11] Y. Li and S. C. Benjamin, *Physical Review X* **7**, 021050 (2017).
- [12] C. Kokail, C. Maier, R. van Bijnen, T. Brydges, M. K. Joshi, P. Jurcevic, C. A. Muschik, P. Silvi, R. Blatt, C. F. Roos, and P. Zoller, *Nature* **569**, 355 (2019).
- [13] S. Endo, J. Sun, Y. Li, S. C. Benjamin, and X. Yuan, *Physical Review Letters* **125**, 010501 (2020).
- [14] C. Ortiz Marrero, M. Kieferová, and N. Wiebe, *PRX Quantum* **2**, 040316 (2021).
- [15] T. L. Patti, K. Najafi, X. Gao, and S. F. Yelin, *Physical Review Research* **3**, 033090 (2021).
- [16] M. Cerezo, A. Sone, T. Volkoff, L. Cincio, and P. J. Coles, *Nat Commun* **12**, 1791 (2021).
- [17] A. V. Uvarov and J. D. Biamonte, *Journal of Physics A: Mathematical and Theoretical* **54**, 245301 (2021).
- [18] S. Wang, E. Fontana, M. Cerezo, K. Sharma, A. Sone, L. Cincio, and P. J. Coles, *Nat Commun* **12**, 6961 (2021).
- [19] A. Pesah, M. Cerezo, S. Wang, T. Volkoff, A. T. Sornborger, and P. J. Coles, *Physical Review X* **11**, 041011 (2021).
- [20] M. Larocca, P. Czarnik, K. Sharma, G. Muraleedharan, P. J. Coles, and M. Cerezo, *Quantum* **6**, 824 (2022).
- [21] S. H. Sack, R. A. Medina, A. A. Michailidis, R. Kueng, and M. Serbyn, *PRX Quantum* **3**, 020365 (2022).
- [22] M. Cerezo, M. Larocca, D. García-Martín, N. L. Diaz, P. Braccia, E. Fontana, M. S. Rudolph, P. Bermejo, A. Ijaz, S. Thanasilp, E. R. Anschuetz, and Z. Holmes, *Nature Communications* **16**, 7907 (2025).
- [23] Y. Shao, F. Wei, S. Cheng, and Z. Liu, *Physical Review Letters* **133**, 120603 (2024).
- [24] A. Angrisani, A. Schmidhuber, M. S. Rudolph, M. Cerezo, Z. Holmes, and H.-Y. Huang, *Physical Review Letters* 10.1103/1h6x-7rc3 (2025).
- [25] V. Martinez, A. Angrisani, E. Pankovets, O. Fawzi, and D. Stilck França, *Physical Review Letters* **134**, 250602 (2025).
- [26] A. A. Mele, *Quantum* **8**, 1340 (2024).
- [27] A. Arrasmith, M. Cerezo, P. Czarnik, L. Cincio, and P. J. Coles, *Quantum* **5**, 558 (2021).
- [28] M. C. Caro, H.-Y. Huang, N. Ezzell, J. Gibbs, A. T. Sornborger, L. Cincio, P. J. Coles, and Z. Holmes, *Nature Communications* **14**, 3751 (2023).
- [29] G. E. Crooks, arXiv 10.48550/arXiv.1905.13311 (2019).
- [30] J. Li, X. Yang, X. Peng, and C.-P. Sun, *Physical Review Letters* **118**, 150503 (2017).
- [31] M. Ragone, B. N. Bakalov, F. Sauvage, A. F. Kemper, C. Ortiz Marrero, M. Larocca, and M. Cerezo, *Nat. Commun.* **15**, 7172 (2024).
- [32] A. V. Uvarov and J. D. Biamonte, *J. Phys. A: Math. Theor.* **54**, 245301 (2021).
- [33] S. Y.-C. Chen and S. Yoo, *Entropy* **23**, 460 (2021).
- [34] M. Sajjan, J. Li, R. Selvarajan, S. Hari Sureshbabu, S. Suresh Kale, R. Gupta, V. Singh, and S. Kais, *Chemical Society Reviews* **51**, 6475 (2022).
- [35] S. Xu and B. Swingle, *PRX Quantum* **5**, 010201 (2024).
- [36] B. Kobrin, T. Schuster, M. Block, W. Wu, B. Mitchell, E. Davis, and N. Y. Yao, *A Universal Protocol for Quantum-Enhanced Sensing via Information Scrambling* (2024).
- [37] J. Romero, J. P. Olson, and A. Aspuru-Guzik, *Quantum Science and Technology* **2**, 045001 (2017).
- [38] D. Bondarenko and P. Feldmann, *Physical Review Letters* **124**, 130502 (2020).
- [39] S. G. Mehendale, B. Peng, N. Govind, and Y. Alexeev, *J. Phys. Chem. A* **127**, 4526 (2023).

- [40] T. Haug, K. Bharti, and M. Kim, PRX Quantum **2**, 040309 (2021).
- [41] B. Collins, S. Matsumoto, and J. Novak, Notices of the American Mathematical Society **69**, 1 (2022).